POLITECNICO DI TORINO
Repository ISTITUZIONALE

Comparison of Equivalent Circuit's Parameters Obtained for Half Cells of PV Mini-Modules Tested under Sunlight and Partial Shading

Original
Comparison of Equivalent Circuit's Parameters Obtained for Half Cells of PV Mini-Modules Tested under Sunlight and Partial Shading / Schubert, S., Malgaroli, G., Ciocia, A., Spertino, F.. - ELETTRONICO. - (2024), pp. 1-6. (2024 International Conference on Smart Energy Systems and Technologies (SEST) Turin (Italy)) [10.1109/SEST61601.2024.10694340].

Availability:
This version is available at: 11583/2997555 since: 2025-02-17T13:16:43Z

Publisher:
IEEE

Published
DOI:10.1109/SEST61601.2024.10694340

Terms of use:

This article is made available under terms and conditions as specified in the corresponding bibliographic description in the repository

Publisher copyright
IEEE postprint/Author's Accepted Manuscript

©2024 IEEE. Personal use of this material is permitted. Permission from IEEE must be obtained for all other uses, in any current or future media, including reprinting/republishing this material for advertising or promotional purposes, creating new collecting works, for resale or lists, or reuse of any copyrighted component of this work in other works.

(Article begins on next page)

28 November 2026

Comparison of Equivalent Circuit's Parameters Obtained for Half Cells of PV Mini-Modules Tested under Sunlight and Partial Shading

Stefano Schubert *Dip. Energia "Galileo Ferraris"*
Politecnico di Torino
Turin, Italy
stefano.schubert@polito.it
Gabriele Malgaroli *Dip. Energia "Galileo Ferraris"*
Politecnico di Torino
Turin, Italy
gabriele.malgaroli@polito.it
Alessandro Ciocia *Dip. Energia "Galileo Ferraris"*
Politecnico di Torino
Turin, Italy
alessandro.ciocia@polito.it

Filippo Spertino *Dip. Energia "Galileo Ferraris"*
Politecnico di Torino
Turin, Italy
filippo.spertino@polito.it

Abstract

This paper aims is included in a line of research aiming to develop an automatic acquisition system for the fault detection in PV plants. The performance of photovoltaic (PV) generators can be modeled using electrical equivalent circuits with parameters ranging from three to seven. This study compares the equivalent circuits to extract the parameters for half-cells of PV modules tested under natural sunlight and partial shading. The tests, conducted at Politecnico di Torino (Italy), reveal that the four-parameter model provides an optimal balance of accuracy and computational efficiency under sunlight, whereas the five-parameter model demonstrates higher accuracy under partial shading. These insights are essential for implementing effective fault detection systems in PV plants to distinguish between faults and suboptimal operating conditions such as partial shading.

Keywords: equivalent circuit's parameters, single diode model, photovoltaic cell, half-cells, fault detection

I. Introduction

The escalating global population and urbanisation have led to a substantial increase in global energy consumption, with a shift from conventional fossil fuels towards Renewable Energy Sources (RES). Among these, PhotoVoltaic (PV) plants and wind farms are the most important thanks to their high reliability and lack of polluting emissions. One area of study in wind farms is figuring out how well wind turbines really work by comparing the readings from special instruments called Supervisory Control and Data Acquisition (SCADA) with what the manufacturers say they can do [1]. Within the PV field, scientists are working on projects aiming to create new PV materials with higher performance, like perovskite [2], to improve the reliability of PV systems by advanced monitoring techniques [3], [4] and the efficiency of conventional PV systems.The performance of PV generators can be modelled by electrical equivalent circuits with a variable number of parameters. The Single Diode Model (SDM) and the Double Diode Model (DDM), which have 5 and 7 parameters, respectively, are the two most popular circuit models [5]. A considerable amount of research has already been performed in this field, mainly regarding the accurate tracking of the Maximum Power Point (MPP) under many irradiance conditions. There are well-known models that use equations to figure out the parameters of an equivalent circuit from the current-voltage (*I-V*) characteristic curve of PV modules [6]. However, over the last 20 years, improved algorithms have been developed in computer technology to numerically extract parameters of equivalent circuits [7]. Actually, numerical optimisation methods are generally required due to the non-linear characteristics of the *I-V* equations for the equivalent circuits [8]. Among these, the most common ones are the genetic algorithm, particle swarm optimisation, simulated annealing, evolutionary algorithms, differential evolution algorithms, and artificial neural networks. Moreover, some papers in the literature investigated different circuits, spanning from the one-parameter to the nine-parameter models [9]. They differ in terms of accuracy and computational cost, and the selection of the most adequate circuit is affected by the individual needs [10]. However, little investigation has been carried out on the effects of partial shading on the parameters of these equivalent circuits.

The focus of existing literature is related to the accuracy improvement of parameters' extraction to better detect the MPP under sunlight, and investigations regarding the performance under shading have not been carried out. This research field aims to build a model permitting automatic diagnostics by the inverters of multi-megawatt PV plants based on the equivalent circuit's parameters. In particular, this future technique will be based on the comparison between the equivalent circuit's parameters extracted in real time by the inverters and reference values, corresponding to healthy arrays. In this context, the model will need to distinguish between faults or failures and feasible but not optimal operating conditions, e.g., mismatch due to partial shading.

This paper compares the equivalent circuit's parameters determined for half cells of ten identical PV modules tested under natural sunlight and under shading at the university campus of Politecnico di Torino (Torino, Italy), determining which performs better under sunlight and mismatch conditions. An indirect procedure was used to determine the *I-V* curve of shaded cells, and the results were obtained for four circuits, with a number of equivalent circuit's parameters between 3 and 7. The structure of the work is the following: Section II will describe the indirect methodology employed to determine the *I-V* curve for shaded cells. Section III presents the equivalent circuits employed in this work and the numerical methodology to extract their parameters. Section IV describes the measurement system used to acquire the experimental data, and Section V includes the results. Finally, Section VI contains the conclusions.

II. Review of Equivalent Circuits from Literature

In literature, many equivalent circuits permit to determine the *I-V* curve of PV generators. Such models differ in terms of number of parameters, complexity, and, thus, computational cost. This section presents the most common equivalent circuits used in literature by highlighting their differences.

A. 3 Parameters Model (3P)

The simplest equivalent circuit is show in Fig. 1: such a model includes three parameters, namely the photogenerated current I_{ph}, which represents the current generation in the p-n junction of the PV modules; the reverse saturation current I_0, which models the losses due to diffusion and recombination in the junction; the diode ideality factor n, which represents the non-ideal behaviour of the p-n junction as a diode[11]. The equation of this equivalent circuit is the following:

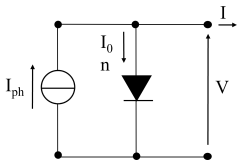

Fig. 1. Equivalent circuit with 3 parameters.

$$I = I_{\text{ph}} - I_{\text{j}} = I_{\text{ph}} - I_0 \cdot (e^{\frac{q \cdot V}{n \cdot k_{\text{B}} \cdot T_{\text{c}}}} - 1) \tag{1}$$

where q is the electron charge ($1.602 \cdot 10^{-19}$ C), k_{B} is the Boltzmann constant ($1.38 \cdot 10^{-23}$ J/K) and T_{c} is the cell temperature. As equation 1 is explicit, a numerical method is not required to determine the points of the *I-V* curve. Indeed, an analytical solution can be obtained starting from the knowledge of the equivalent circuit's parameters, requiring a negligible computational effort.

B. 4 Parameters Model (4P)

The equivalent circuit with 4 parameters (Fig. 2) includes one additional parameter[12], the series resistance R_{s}[13], which takes into account ohmic losses due to the presence of frontal electrical contacts (busbars and fingers) in PV modules[14]. This term is, generally, low (i.e., a few mΩ per solar cell), and the equation of the circuit is the following:

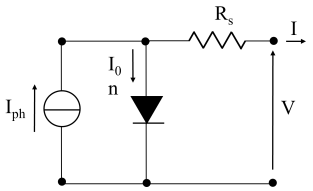

Fig. 2. Equivalent circuit with 4 parameters.

$$I = I_{\text{ph}} - I_{\text{j}} = I_{\text{ph}} - I_0 \cdot (e^{\frac{q \cdot (V + R_{\text{s}} \cdot I)}{n \cdot k_{\text{B}} \cdot T_{\text{c}}}} - 1) \tag{2}$$

The presence of the series resistance in the model complicates the solution of the equation. Actually, equation 2 is implicit, and an analytical solution of the problem is not possible. Hence, starting from this model, a numerical algorithm is necessary to solve the implicit equation, with a significantly increased computational time with respect to the 3-parameters model.

C. 5 Parameters Model (5P)

The equivalent circuit with 5 parameters, namely "Single Diode Model" (SDM) (Fig. 3), is the most common and, generally, represents a good compromise between simplicity, high accuracy and low computational cost. With respect to the 4-parameters model, this circuit includes one additional resistor, the shunt resistance R_{sh}, which takes into account leakage currents through the lateral surfaces of PV cells. This term is, generally, high (i.e., tens or hundreds Ω), and its contribution can be neglected in most of applications [15]. The equation of the 5P is the following[16]:

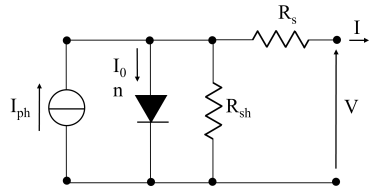

Fig. 3. Equivalent circuit with 5 parameters.

$$I = I_{\text{ph}} - I_0 \cdot (e^{\frac{q\cdot(V+R_{\text{s}}\cdot I)}{n\cdot k_{\text{B}}\cdot T_{\text{c}}}} - 1) - (V + R_{\text{s}} \cdot I)/R_{\text{sh}} \quad (3)$$

D. 7 Parameters Model (7P)

With respect to the 5P, the equivalent circuit with 7 parameters, namely "Double Diode Model" (DDM) (Fig. 4) introduces one additional diode to separately take into account the effects due to diffusion and recombination in the p-n junction. In literature, this model is, generally, preferred in case of mismatch, e.g., due to partial shading, or, in general, in case of low irradiance [17][18]. The equation of the 7P is the following:

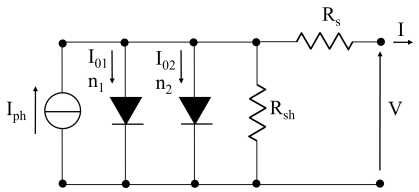

Fig. 4. Equivalent circuit with 7 parameters.

$$I = I_{\text{ph}} - I_{0,1} \cdot (e^{\frac{q\cdot(V+R_{\text{s}}\cdot I)}{n_1\cdot k_{\text{B}}\cdot T_{\text{c}}}} - 1) - I_{0,2} \cdot (e^{\frac{q\cdot(V+R_{\text{s}}\cdot I)}{n_2\cdot k_{\text{B}}\cdot T_{\text{c}}}} - 1) - (V + R_{\text{s}} \cdot I)/R_{\text{sh}} \quad (4)$$

III. Method for the Evaluation of the *I-V* Curve of a Shaded Cell

This work aims to obtain the equivalent circuit's parameters for one shaded cell in 10 PV modules. An indirect method is used to obtain the I-V curve of the shaded cell starting from the knowledge of the curve for the PV module and is presented in [19]. The method, known as "One Module (or One String), Two Tests", requires the measurement of two I-V curves for one PV module or string consisting of N_{s} series-connected cells under natural sunlight. For this activity, a high level of solar irradiance is suggested, i.e., higher than 800 W/m^2. In the first acquisition, the module or the string are uniformly irradiated under natural sunlight ("N_{s} irradiated cells"). On the contrary, the second test involves the measurement of the module or string with $(N_{\text{s}} - 1)$ irradiated cells and one shaded cell ("1 shaded cell and $N_{\text{s}} - 1$ irradiated cells").

The two acquisitions are suggested to be performed in a very short time (maximum suggested interval: a couple of minutes) to reduce fluctuations of environmental parameters (cell temperature T_{c} and irradiance G). After the two measurements, the method consists of the following steps:

- Evaluation of the curve for the module with $(N_{\text{s}} - 1)$ irradiated cells. The *I-V* curve of one cell can be determined by dividing the *I-V* characteristic of the string or module by the number of series-connected cells. In this case, the *I-V* curve of the module with $(N_{\text{s}} - 1)$ irradiated cells can be derived by the following proportional assumption:

$$V_{\text{Ns-1}} = V_{\text{Ns}} \cdot (N_{\text{s}} - 1)/N_{\text{s}} \tag{5}$$

where V_{Ns} and $V_{\text{Ns-1}}$ are the voltage of the module with N_{s} and $N_{\text{s}} - 1$ irradiated cells, respectively.

- Correction of the curve for the module with N_{s} irradiated cells. In order to obtain I-V curves measured in the same environmental conditions, the data for the module with N_{s} irradiated cells (measured conditions) were corrected to the environmental conditions in which the curves of the modules with $(N_{\text{s}} - 1)$ irradiated cells and one shaded cell were obtained (corrected conditions). Such a correction was performed according to the following equations:

$$I_{\text{corr}} = I_{\text{m}} + I_{\text{sc,m}} \cdot \left(\frac{G_{\text{corr}}}{G_{\text{m}}} - 1 \right) + \alpha \cdot (T_{\text{corr}} - T_{\text{m}}) \tag{6}$$

$$V_{\text{corr}} = V_{\text{m}} - R_{\text{s,m}} \cdot (I_{\text{corr}} - I_{\text{m}}) - k \cdot I_{\text{corr}} \cdot (T_{\text{corr}} - T_{\text{m}}) + \beta \cdot (T_{\text{corr}} - T_{\text{m}}) \tag{7}$$

where:

  - I_{corr} is the current at corrected environmental conditions.
  - I_{m} is the measured current.
  - $I_{\text{sc,m}}$ is the measured short circuit current.
  - V_{corr} is the voltage at corrected environmental conditions.
  - V_{m} is the measured voltage.
  - R_{s} is the series resistance of the module.
  - G_{corr} is the corrected irradiance.
  - G_{m} is the measured irradiance.
  - T_{corr} is the corrected cell temperature.
  - T_{m} is the measured temperature.
  - α is the thermal coefficient of the current (0.045%/°C).
  - β is the thermal coefficient of the voltage (-0.275%/°C).
  - k is a correction parameter.

- Evaluation of the *I-V* curve for the shaded cell. The curve of one shaded cell is obtained by subtracting, for the same current, the voltages between the curve of $(N_{\text{s}} - 1)$ irradiated cells and one shaded cell (subscript "1s"), and the curve of $(N_{\text{s}} - 1)$ irradiated cells. Before subtracting the curves, an interpolation is performed on the current: the currents of the *I-V* curve with $N_{\text{s}} - 1$ irradiated cells are interpolated to match the values of the 1s curve. Hence, for each ith current value of these curves (I_{i}), the voltage of the shaded cell $V_{\text{sh,i}}$ is obtained as follows:

$$V_{\text{sh,i}} = V_{\text{1s,i}} - V_{\text{(Ns-1),i}} \tag{8}$$

IV. Description of the Acquisition System

A. PV modules under test

In this work, the I-V curve of one shaded cell for 10 flexible photovoltaic modules consisting of 4 half-cells (Fig. 6) is obtained with the method presented in the previous section. At STC, these modules have an open-circuit voltage of 2.6 V, a short-circuit current of 4 A and a maximum power of 6.2 W. In addition, the equivalent circuit's parameters are extracted for each cell, with statistical evaluation of the repeatability.

B. Description of the acquisition system

The data acquisition system used at Politecnico di Torino for the measurement of the *I-V* curves PV modules is composed of the following devices:

- one RTD sensor to measure the temperature of PV cells on their rear side (T_m) with uncertainty of $\pm 0.26\%$.
- one secondary standard pyranometer, used to detect the solar irradiance incident on PV modules (G) with uncertainty of $\pm 1.42\%$.
- one *Electronic Load* HH PLA 812 (maximum power of 800 W, resolution of 16 bits, sampling rate of 1 kSa/s, uncertainty ¡ $\pm 0.2\%$ on current and voltage) is used as a resistor with variable resistance to acquire the current and voltage signals from PV modules.
- one NI-9216 module (resolution of 24-bit, and sample rate of 50 Sa/s) receiving the signal from the RTD sensors, and one NI-9219 module (resolution of 24-bit, and sampling rate of 100 Sa/s) receiving the signal from the pyranometer. These modules are connected to one *NI-CompactDAQ* board, with four slots and equipped with a USB interface.
- one *PC* running a LabVIEW software to manage the acquisition of the electrical and environmental signals.

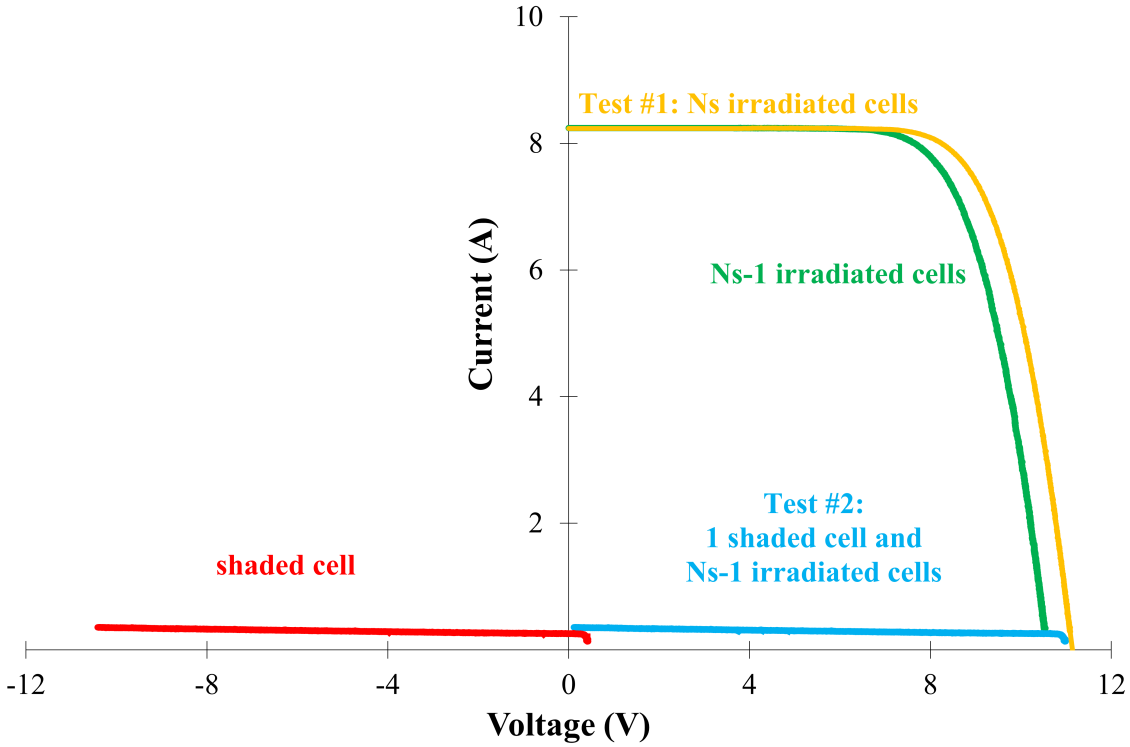

Fig. 5. I-V curves used in the method to evaluate that of the shaded cell

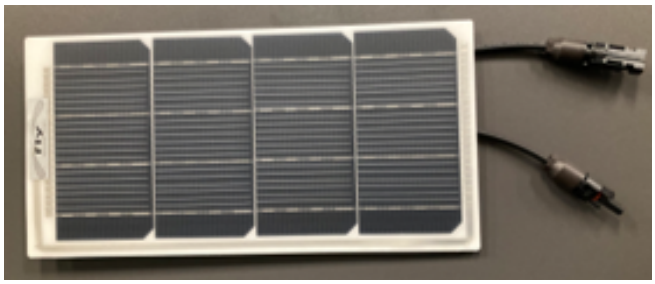

Fig. 6. Picture for one out of the 10 PV modules under test.

C. Extraction of equivalent circuit's parameters

In this work, the Differential Evolution algorithm is used to extract the parameters of the 4-parameters model, of the SDM and DDM. This method is a stochastic population based method used for global optimization problems. At each step, the method selects a trial candidate by mixing each candidate solution with others. Many strategies are available to create trial candidates: in this work, the 'best1bin' strategy is adopted, in which two members of the population are randomly chosen and their difference is used to mutate the best member. This method does not evaluate the gradient to identify the minimum of the objective function, and can search large areas of candidate space, but a high number of function evaluations is, generally, required. A trial vector is then constructed and its fitness is compared with the original candidate: the best candidate replaces the old one. In this work, a maximum number of iterations equal to 1000 and a tolerance of 1% are set.

V. Results

The equivalent circuit's parameters were extracted for 10 flexible photovoltaic modules consisting of 4 half-cells under natural sunlight and under partial shading. In particular, the parameters were numerically determined for four models: the 3P (I_{ph}, I_0, n), 4P ($I_{\text{ph}}, I_0, n, R_{\text{s}}$), 5P ($I_{\text{ph}}, I_0, n, R_{\text{s}}, R_{\text{sh}}$), and the 7P ($I_{\text{ph}}, I_{0,1}, n_1, I_{0,2}, n_2, R_{\text{s}}, R_{\text{sh}}$). The results from these models were compared to identify the circuit with best compromise between high accuracy and low computational time under sunlight and under shading, and table I reports the median values for the Root Mean Square Error ($RMSE$), the deviation at the Maximum Power Point (MPP) and the computational effort for ten modules analyzed, divided by mathematical model. The 3P was the least accurate model in both conditions, with a median $RMSE$ of 2.02% and 15.8 % and a median deviation at

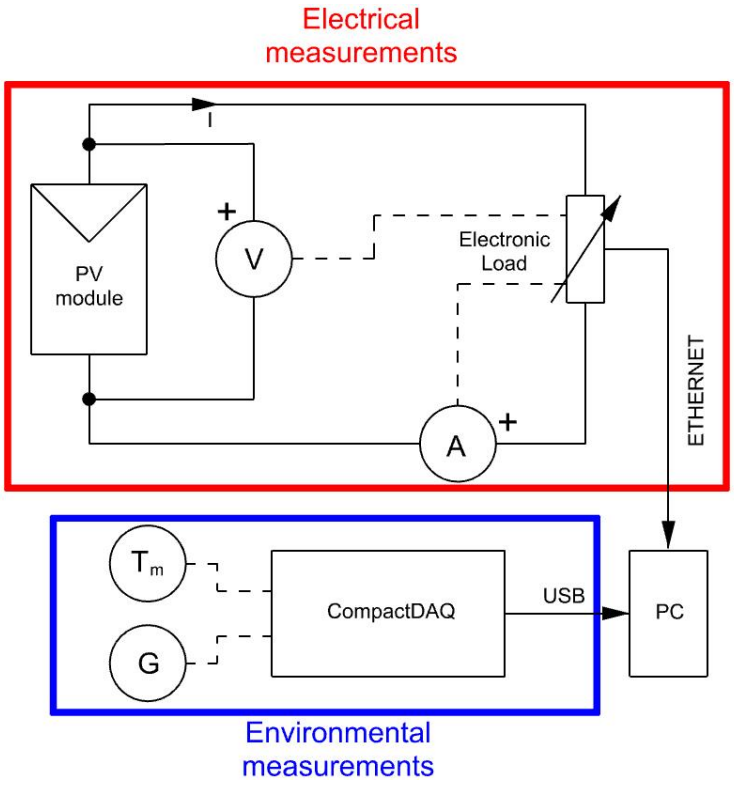

Fig. 7. Scheme of the acquisition system

MPP of 5.54 % and 3.24 % under sunlight and partial shading, respectively. Fig.10 confirms these values as it presents the *I-V* curves of the same single cell of module number 2, all under high solar radiation, modelled with the equivalent parameters and from experiments: the 3P curve is the worse and the farthest from the measurements. On the contrary, the computational time required to extract its parameters was the lowest ($<$ 1s for both conditions).

Despite the 7P required the highest computational effort ($>$ 15 s for each parameters extraction), the accuracy of its results was not the best for any condition. As expected, under sunlight, the median $RMSE$ and deviation at MPP obtained for the 7P were the lowest, being 0.61 % and 1.81 %, respectively; however, these results were comparable with that of 4P and 5P. In addition, the 7P results were not the best in the partial shading scenario as the 5P achieved lower median $RMSE$ and deviation at MPP (0.9 % and 0.796 %, respectively). Hence, such results do not justify the adoption of the 7P for real fault detection applications since its requires the highest computational effort but its results were comparable with other models under sunlight and they were not the best under partial shading.

The median $RMSE$ and deviation at MPP of the 4P and 5P were comparable under sunlight ($\approx$ 0.68 % and 2 % for both the models), but the computational time of the 5P was almost double that of 4P ($\approx$ 8 s vs. 4 s). Hence, under sunlight condition, the 4P was the optimal compromise as its results showed almost the best accuracy and a reasonably low computational time. Under partial shading, the performance of the 4P was closer to that of 3P rather than that of 5P. Fig.11 depicts the *I-V* curves modeled with the extracted parameters, as well as the measured *I-V* curve under mismatch; the cell is the same showed in 10. In this case, the approximation of the 4P curve is as bad as that of 3P as the absence of the R_{sh} has a significant impact in case of shading. Actually, despite its median deviation at MPP was comparable with that of 5P ($\approx$ 0.7 %), its $RMSE$ was about five times higher than that of 5P. Thus, under shading, the 5P represented a better match rather than 4P as it provided a much better accuracy for the overall *I-V* curve with an acceptable computational effort.

In Fig.8 and Fig.9, the distributions of errors at the MPP and the RMSE for the PV modules under natural sunlight and partial shading, respectively, are shown. The two figures consist in a matrix of plots: the diagonal plots provide the kernel density estimations of RMSE, error at MPP and execution time, while the off-diagonal plots present the correlations between two out of the three parameters. Regarding the $RMSE$ - computational time and the deviation at MPP - computational time plots, the optimal model would provide results in bottom left corner of the figures, which corresponds to high accuracy and low execution time. According to this interpretation of the plots, the 3P and 7P models results are far from the optimal region due to low accuracy (3P) and high computational effort (7P) for both conditions. On the contrary, the 4P model is the optimal in the sunlight scenario as its results are the closest to the optimal region of the plots.

Regarding the partial shading condition, the results present in Fig.9 delineate a different interpretation. Indeed, the $RMSE$ distribution for the 4P is sparse, with its median exceeding that of the 3P. Despite the distribution of the deviation at MPP is

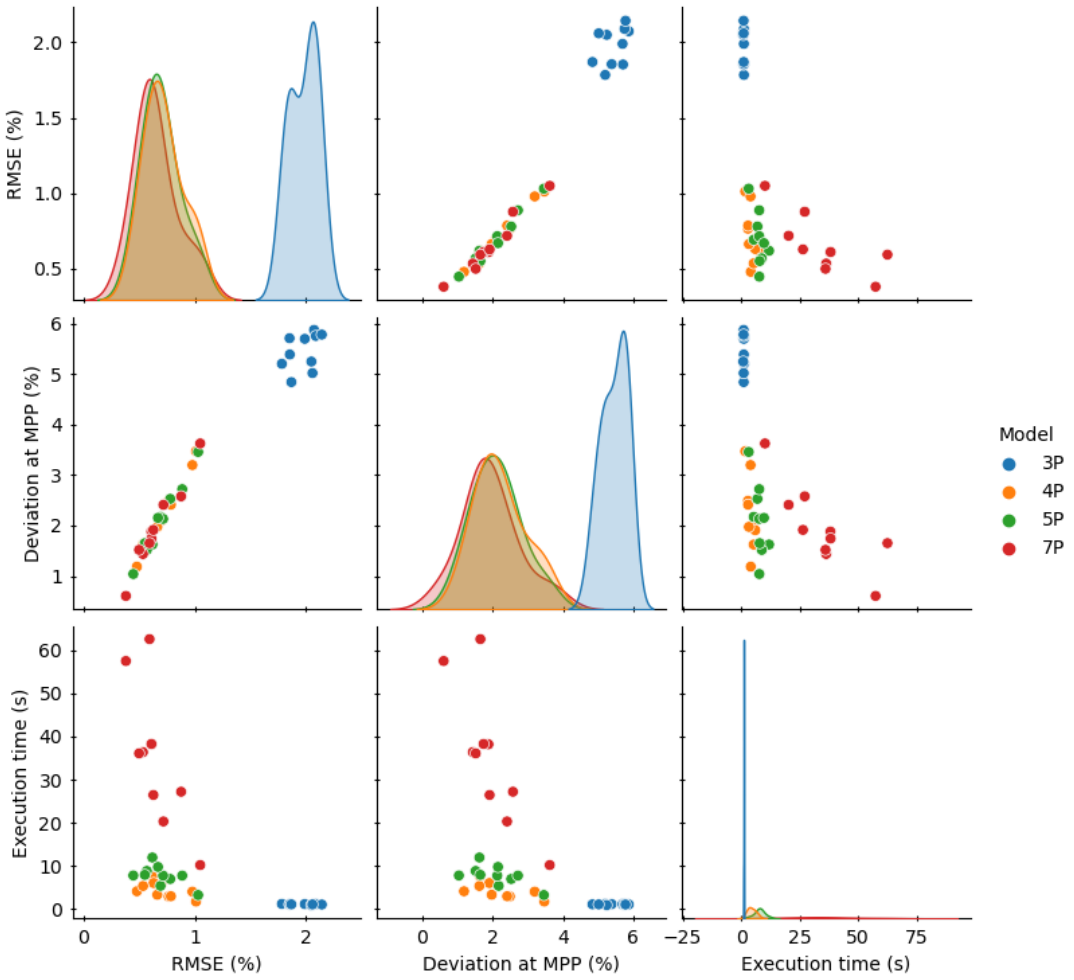

Fig. 8. Distributions for the modules under sunlight.

TABLE I
MEDIAN RESULTS FOR THE MODULES UNDER SUNLIGHT AND PARTIAL SHADING

Modules under sunlight

Parameter	3P	4P	5P	7P
RMSE (%)	2.02	0.681	0.68	0.61
Deviation at MPP (%)	5.54	2.04	2.14	1.81
Execution time (s)	1.11	4.1	7.79	36.2

Modules under partial shading

Parameter	3P	4P	5P	7P
RMSE (%)	3.24	5.59	0.9	0.904
Deviation at MPP (%)	15.8	0.751	0.796	1.07
Execution time (s)	0.832	1.4	4.44	15.9

comparable to that of 5P, the prediction of the *I-V* curve with the 4P model is much worse. Hence, under partial shading, the 5P is the optimal model with the best trade off between low computational cost and high accuracy of parameters extraction. In the future the method used in this study will be tested on more photovoltaic modules built with different technologies to further validate and potentially enhance its effectiveness.

VI. CONCLUSIONS

The presented paper contributes to the field of photovoltaic (PV) research by exploring the potential of using equivalent circuits' parameters for automatic fault detection of PV plants. In particular, this study investigates the applicability of different equivalent circuits to extract the parameters for half cells of ten identical monocrystalline silicon PV modules tested under natural sunlight and partial shading. Results indicate that the four-parameters (4P) model outperforms the five-parameters (5P)

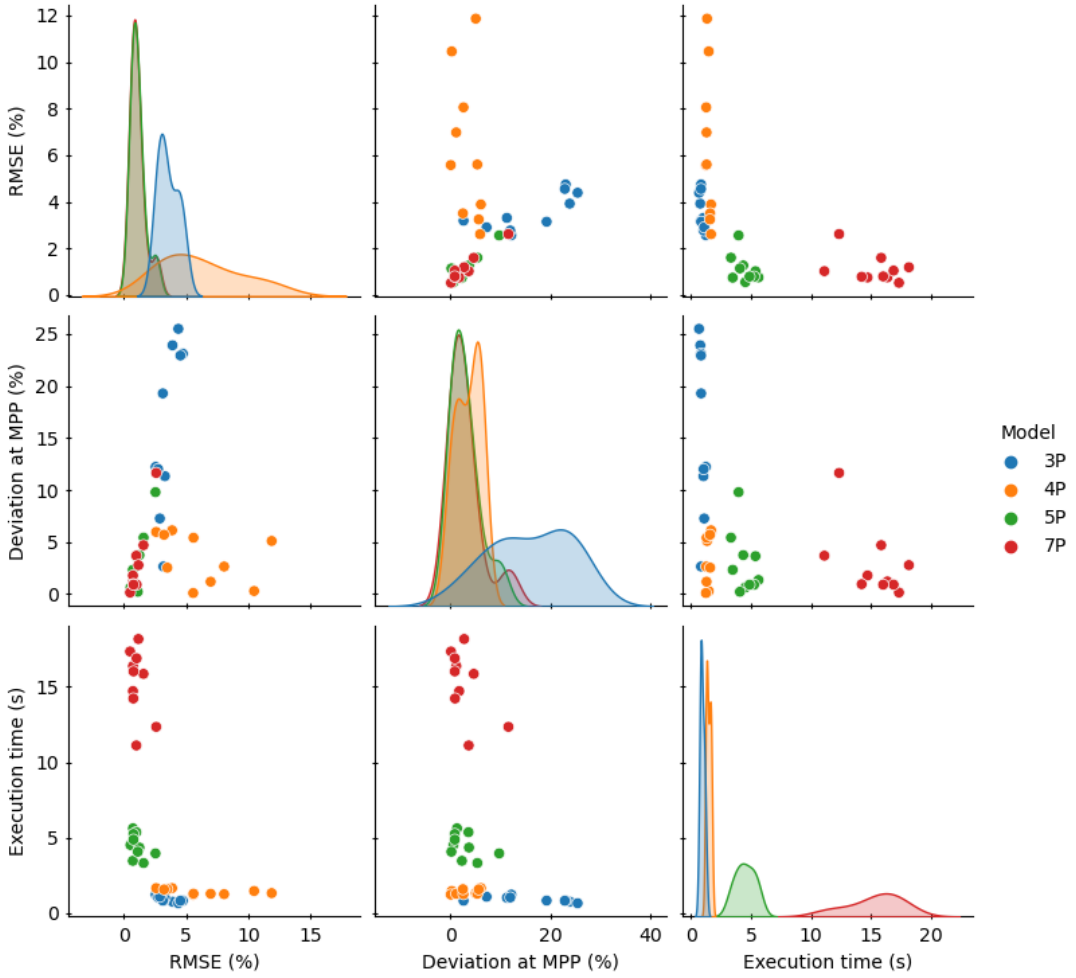

Fig. 9. Distributions for the modules under partial shading.

model, being the optimal compromise between high accuracy and low computational time under sunlight. Indeed, the 4P provides median Root Mean Square Errors ($RMSEs$) and deviations at MPP comparable to that of more complex models ($\approx$ 0.7 % and 2 %, respectively), with reasonably low computational effort of each parameters extraction ($\approx$ 4s). On the contrary, the optimal model for the partial shading condition is the 5P as it provides higher accuracy than the 4P, with median $RMSE$ and deviation at MPP of $\approx$ 0.9 % and 0.8 %, respectively. The integration of the 3P and the 7P in real fault detection applications is not possible due to a too low accuracy (3P) or a too high computational time (7P). This information will be used in future works to develop an algorithm for fault detection in PV plants: this algorithm will be based on 4P model under sunlight and 5P model under partial shading to distinguish between faults and sub-optimal operating conditions.

References

[1] A. Carullo, A. Ciocia, P. Di Leo, F. Giordano, G. Malgaroli, L. Peraga, F. Spertino, and A. Vallan, "Comparison of correction methods of wind speed for performance evaluation of wind turbines," 2020, p. 291 – 296.

[2] G. Aime, A. Ciocia, G. Malgaroli, S. Narbey, L. Saglietti, and F. Spertino, "Degradation assessment for prototypal perovskite photovoltaic modules in long term outdoor experimental campaign," *Proceedings - 2023 IEEE International Conference on Environment and Electrical Engineering and 2023 IEEE Industrial and Commercial Power Systems Europe, EEEIC / I and CPS Europe 2023*, 2023.

[3] F. Bizzarri, S. Nitti, and G. Malgaroli, "The use of drones in the maintenance of photovoltaic fields," *E3S Web of Conferences*, vol. 119, p. 21, 2019.

[4] A. Ciocia, A. Carullo, P. DI Leo, G. Malgaroli, and F. Spertino, "Realization and Use of an IR Camera for Laboratory and On-field Electroluminescence Inspections of Silicon Photovoltaic Modules." Institute of Electrical and Electronics Engineers Inc., 2019.

[5] G. C. Seritan, B.-A. Enache, F.-C. Adochiei, F.-C. Argatu, C. Christodoulou, V. Vita, A. R. Toma, C. H. Gandescu, and F.-I. Hathazi, "Performance evaluation of photovoltaic panels containing cells with different bus bars configurations in partial shading conditions," *Rev. Roum. Sci. Tech.-Ser. Electrotech. Energetique*, vol. 65, pp. 67–70, 2020.

[6] N. Araújo, F. Sousa, and F. Costa, "Equivalent models for photovoltaic cell–a review," *Revista de Engenharia Térmica*, vol. 19, no. 2, pp. 77–98, 2020.

[7] B. Maniraj and A. P. Fathima, "Parameter extraction of solar photovoltaic modules using various optimization techniques: A review," in *Journal of Physics: Conference Series*, vol. 1716, no. 1. IOP Publishing, 2020, p. 012001.

[8] M. N. Mohammedali, M. Rasheed, S. Shihab, T. Rashid, Saad, and A. Hamad, "Fuzzy set technique application: The solar cell," 2021. [Online]. Available: https://api.semanticscholar.org/CorpusID:235842112

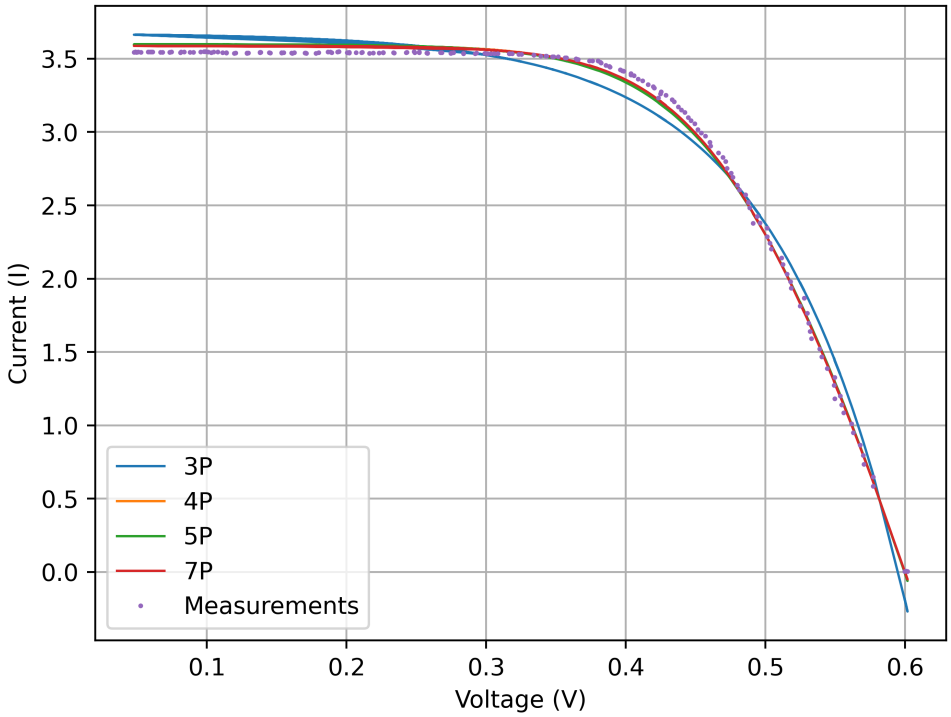

Fig. 10. Measured *I-V* curve alongside the calculated *I-V* curves using the equivalent circuit parameters under sunlight, for one cell of module #2.

[9] H. Rezk and M. A. Abdelkareem, "Sciencedirect optimal parameter identification of triple diode model for solar photovoltaic panel and cells," pp. 10–12, 2021. [Online]. Available: www.sciencedirect.comwww.elsevier.com/locate/

[10] R. Venkateswari and N. Rajasekar, "Review on parameter estimation techniques of solar photovoltaic systems," *International Transactions on Electrical Energy Systems*, vol. 31, no. 11, p. e13113, 2021.

[11] A. N. Yassien, A. Elnozahy, and A. M. Abdelshafy, "Parameter extraction of single diode pv module based on hybrid pso–gwo algorithm," *2023 24th International Middle East Power System Conference (MEPCON)*, pp. 1–6, 2023. [Online]. Available: https://api.semanticscholar.org/CorpusID:268546418

[12] A. R. Jordehi, "Parameter estimation of solar photovoltaic (pv) cells: A review," *Renewable and Sustainable Energy Reviews*, vol. 61, pp. 354–371, 2016.

[13] M. Rasheed and S. Shihab, "Modelling and parameter extraction of pv cell using single-diode model," 2020. [Online]. Available: https://api.semanticscholar.org/CorpusID:226273824

[14] L. Nouri, F. Z. Ihfa, Y. A. Oubella, Z. Sakhi, and M. Bennai, "Single-diode multi-junction solar cell models five-parameter estimation method," *Indian Journal of Physics*, pp. 1–9, 2023. [Online]. Available: https://api.semanticscholar.org/CorpusID:259853175

[15] A. Gholami, M. Ameri, M. Zandi, and R. G. Ghoachani, "Electrical, thermal and optical modeling of photovoltaic systems: Step-by-step guide and comparative review study," *Sustainable Energy Technologies and Assessments*, 2022. [Online]. Available: https://api.semanticscholar.org/CorpusID:244067387

[16] S. Hara, H. Douzono, M. Imamura, and T. Yoshioka, "Estimation of photovoltaic cell parameters using measurement data of photovoltaic module string currents and voltages," *IEEE Journal of Photovoltaics*, vol. 12, pp. 540–545, 2021. [Online]. Available: https://api.semanticscholar.org/CorpusID:242348256

[17] P. Maric, I. Marasović, I. Bevanda, and T. Betti, "Extraction of pv module electrical parameters based on the single diode and double diode model of a pv cell," *2022 7th International Conference on Smart and Sustainable Technologies (SpliTech)*, pp. 01–05, 2022. [Online]. Available: https://api.semanticscholar.org/CorpusID:251705432

[18] M. I. Ghoto, M. H. Balouch, T. A. Jummani, and A. A. Memon, "Parameters extraction of photovoltaic cells using swarm intelligence based optimization technique: research on single diode model and double diode model," *Mehran University Research Journal of Engineering and Technology*, 2023. [Online]. Available: https://api.semanticscholar.org/CorpusID:257941657

[19] A. Ciocia, P. Di Leo, S. Fichera, F. Giordano, G. Malgaroli, and F. Spertino, "A novel procedure to adjust the equivalent circuit parameters of photovoltaic modules under shading," pp. 711–715, 2020.

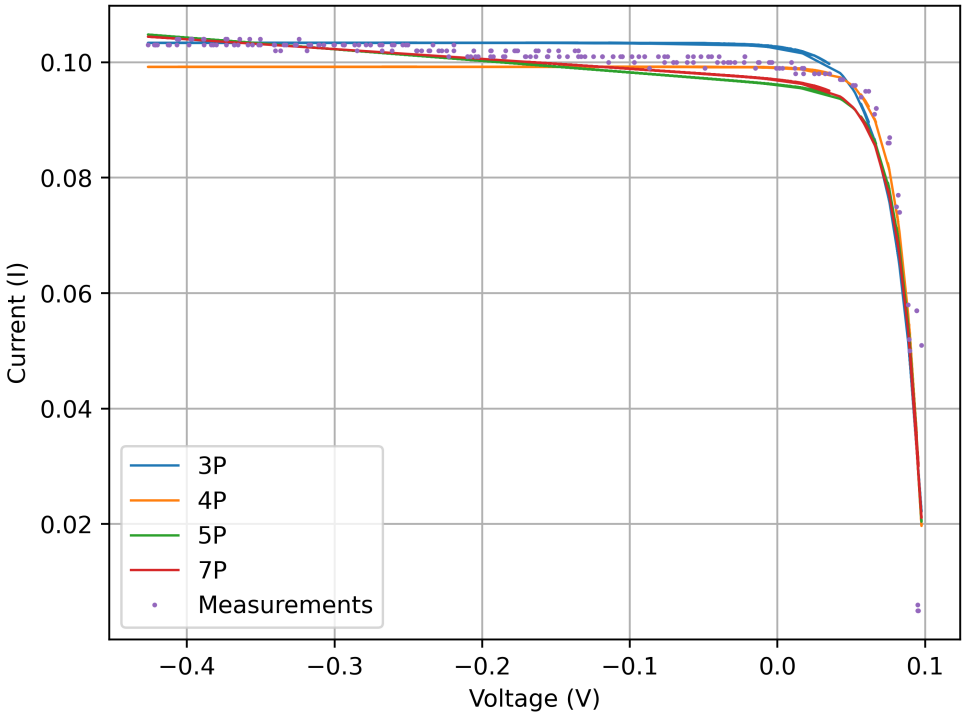

Fig. 11. Measured *I-V* curve alongside the calculated *I-V* curves using the equivalent circuit parameters under shading, for one cell of module #2.